photonics

IMPACT FACTOR 2.1

CITESCORE 2.6

Review

Optical Link Design for Quantum Key Distribution-Integrated Optical Access Networks

Sunghyun Bae and Seok-Tae Koh

Special Issue

Optical Signal Processing for Advanced Communication Systems

Edited by

Dr. Weile Zhai

MDPI

https://doi.org/10.3390/photonics12050418

photonics

MDPI

Review

Optical Link Design for Quantum Key Distribution-Integrated Optical Access Networks

Sunghyun Bae [1,2] and Seok-Tae Koh [3,*]

[1] Department of Electronics Information & Communication Engineering, Kangwon National University, Samcheok 25913, Republic of Korea; baesh@kangwon.ac.kr or sungbae@sejong.ac.kr
[2] Department of AI Convergence Electronic Engineering, Sejong University, Seoul 05006, Republic of Korea
[3] School of Electrical Engineering, Chungbuk National University, Cheongju 28644, Republic of Korea
* Correspondence: seoktae.koh@chungbuk.ac.kr

Abstract: To achieve commercial scalability, fiber-based quantum key distribution (QKD) systems must be integrated into existing optical communication infrastructures, rather than deployed exclusively on dedicated dark fibers. Integrating QKD into optical access networks (OANs) would be particularly advantageous, as these networks provide direct connectivity to end users for whom security is critical. Such integration can address the inherent security vulnerabilities in current OANs, which are primarily based on time-division multiplexing passive optical networks (TDM-PONs). However, integrating QKD into PONs poses significant challenges due to Raman noise and other detrimental effects induced by PON signals, which intensify as the launched power of PONs increases to support higher transmission speeds. In this study, we review recent advancements in both QKD and access network technologies, evaluate the technical feasibility of QKD-OAN integration, and propose cost-effective strategies to facilitate the widespread deployment of QKD in future access networks.

Keywords: quantum key distribution; optical access network; passive optical network

1. Introduction

The rapid expansion of artificial intelligence (AI)-driven services such as ChatGPT-4o, cloud computing, and wireless communications has significantly increased data traffic within optical access networks (OANs) [1–8]. OANs deliver Internet services to multiple end-users through fiber-to-the-x (FTTx) technologies, primarily implemented as passive optical networks (PONs) that operate without optical amplifiers [1–6]. These networks typically support transmission distances of 20–40 km using a time-division multiplexed/time-division multiple access (TDM/TDMA) scheme [1,3–5]. For simplicity, this paper refers to such networks as TDM-PONs instead of TDM/TDMA-PONs [1]. In a TDM-PON, an optical line terminal (OLT) communicates with optical network units (ONUs) by assigning different time slots to each user [1]. A key advantage of this approach is that the branching point, or distribution cabinet, can be implemented using a simple power splitter, significantly reducing costs [6,9]. However, a major drawback of TDM-PONs is their high power budget requirement, as splitting loss increases with the number of ONUs [2]. This issue becomes particularly critical at a line rate exceeding 10 Gb/s [3–8]. For example, the 10 Gb/s symmetric XGS-PON, standardized in the International Telecommunication Union Telecommunication Standardized Sector (ITU-T) G.9807.1, requires a power budget of at least 28 dB to support a 20 km distance with 32 ONUs [10]. In this standard, bidirectional

check for updates

Received: 3 March 2025
Revised: 24 March 2025
Accepted: 23 April 2025
Published: 27 April 2025

Citation: Bae, S.; Koh, S.-T. Optical Link Design for Quantum Key Distribution-Integrated Optical Access Networks. *Photonics* **2025**, *12*, 418. https://doi.org/10.3390/photonics12050418

communication is achieved using a 1577 nm wavelength for downstream (DS) transmission and a 1270 nm wavelength for upstream (US) transmission [10]. Looking ahead, ITU-T Q2/15 and G.Sup64 standardization indicate that future high-speed PONs (HSPs) will likely be based on 25 or 50 Gb/s TDM-PONs or $N \times 50$ Gb/s time-and-wavelength-division multiplexing (TWDM)-PONs [1,4,11,12], following the NG-PON2 (ITU-T G.989) framework [2].

Beyond increasing transmission speeds, security has emerged as a critical concern for OANs which directly connect end users [9,13–16]. With the advent of autonomous vehicles, this security challenge may become a matter of life and death [16–18]. As OANs increasingly encompass mobile fronthaul applications, ensuring their secure operation would become imperative [19,20]. Although TDM- and TWDM-PONs are vulnerable to security threats due to the broadcast nature of DS transmission [13], where signals are shared among multiple ONUs (including unintended recipients), quantum key distribution (QKD) technology can offer unconditional security [14,21,22]. However, the high cost of QKD remains a major barrier to its deployment in OANs, which are highly cost-sensitive [1–9]. In addition, the QKD can be operated in the presence of the Raman scattering induced by PON signals and the distribution loss associated with the point-to-multipoint (P2MP) topology [14,15,23].

In this paper, we provide a comprehensive review of the integration of QKD into OANs. The present review aims to clarify the implementation challenges that arise when integrating QKDs into OANs to enhance security. Previous research suggests that DS continuous-variable (CV)-QKD is a viable option for integration into PONs, particularly in terms of the number of subscribers that can be supported by QKD services. Section 2 reviews the existing PON standards, while Section 3 examines the research on QKD in P2MP topologies. Section 4 suggests a framework for integrating DS CV-QKD with OANs and discusses key implementation challenges in CV-QKD. Section 5 presents the conclusions.

2. High-Speed PON

To successfully integrate QKD into PONs, a comprehensive understanding of PON architectures and their operational constraints is essential. As data rates of PON systems have increased in recent years, the launched power has also been increased to meet the power budget requirements. This has led to an increase in Raman scattering and four-wave mixing (FWM), which has, in turn, degraded the QKD signal quality. It is imperative for researchers in QKD to recognize that the launched power of PON signals cannot simply be reduced to accommodate QKD transmission requirements. To provide a clear understanding of these challenges, this chapter reviews high-speed PON technologies in detail.

2.1. Towards a Beyond-10G-Class TDM-PON

Figure 1a illustrates the DS transmission in a TDM-PON. A TDM signal is transmitted from an OLT to all connected ONUs via a power splitter. Each ONU extracts its designated data while discarding the rest. For the US transmission, as depicted in Figure 1b, ONUs transmit data within their assigned time slots, necessitating a scheduling mechanism. The widespread adoption of a TDM-PON in OANs is primarily driven by its cost-effectiveness, which stems from the use of standard fixed-wavelength optical transceivers for each direction (i.e., DS or US) and a power splitter for signal distribution [3]. Widely deployed symmetric 10G-class TDM-PONs have been standardized by the Institute of Electrical and Electronics Engineers (IEEE) and the Full-Service Access Network (FSAN) and ITU-T, and are referred to as XGS-PON [10] and 10-Gigabit Ethernet PON (EPON) [24], respectively.

For all PONs operating at 10 Gb/s or lower, DS signals are transmitted over the C-band and S-band, while US signals are transmitted over the O-band (see Table 1) [5].

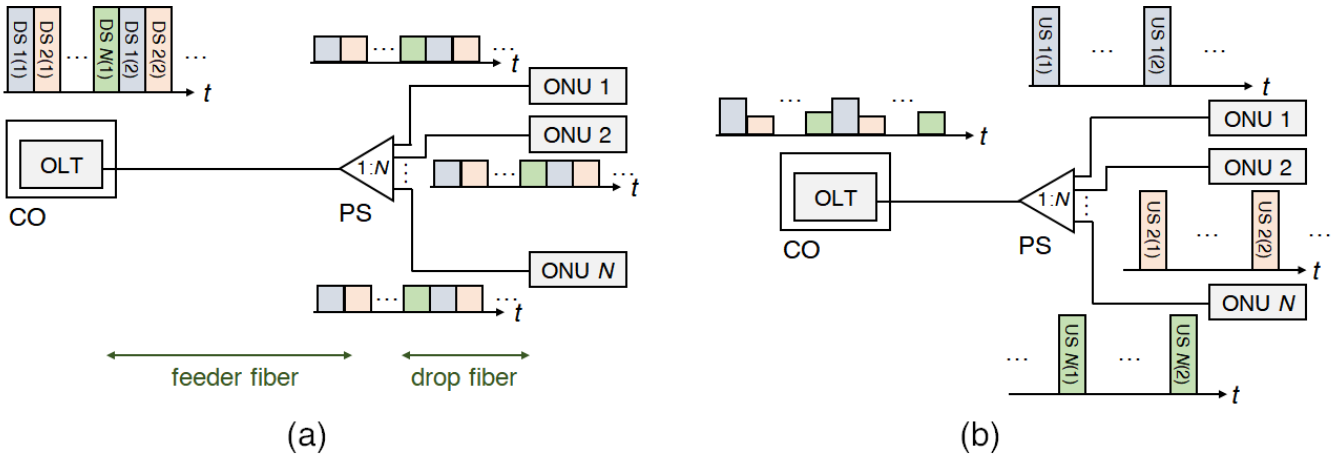

Figure 1. (**a**) DS and (**b**) US transmission in TDM-PON. (CO: central office, PS: power splitter).

The IEEE 802.3ca has standardized the 25G EPON to address the growing bandwidth demands [5]. With the implementation of 100 Gb/s Ethernet, the commercialization of 25 GHz transmitters, such as electro-absorption modulated laser (EML) or directly modulated laser, along with 25 GHz avalanche photodiodes (APDs), has become feasible. However, higher line rates have posed new challenges in maintaining the required 29 dB power budget, which is essential for delivering Internet services to 32–128 ONUs in a TDM-PON. This challenge arises from an additional 5 dB receiver sensitivity penalty, induced by the increased line rate from 10G to 25G [5]. To mitigate this issue, forward error correction (FEC) has been enhanced, APD noise levels have been reduced, and the launched power has been increased to as high as 10.5 dB [25], compensating for the penalty by 1 dB, 1 dB, and 3 dB, respectively [5]. The stringent power budget constraints necessitate the use of on-off-keying (OOK) modulation [3–5]. Additionally, due to the significant chromatic dispersion (CD) penalties at 25G after 20 km of standard single-mode fiber (SSMF), the US wavelength has been shifted to the 1358 nm region (see Table 1).

Table 1. Wavelength plan for PON.

PON Standard	DS Wavelength (nm)	US Wavelength (nm)
GPON (ITU-T G.984) [26]	1480–1500	1290–1330
EPON (IEEE 802.3ah) [27]	1480–1500	1260–1360
XG-PON1 (ITU-T G.987) [28]	1575–1580	1260–1280
XGS-PON (ITU-T G.9807.1) [10]	1575–1580	1260–1280
25G EPON (IEEE 802.3ca) [29]	1340–1342, 1358–1360	1260–1280, 1290–1310, 1319–1321
50G PON (ITU-T G.9804) [11]	1340–1344	1260–1280, 1290–1310
NG-PON2 (ITU-T G.989) [30]	1596–1603	1524–1544

The ITU-T has initiated efforts to standardize the 50G-class PONs [4]. It is anticipated that 50G PONs will require OOK modulation, semiconductor optical amplifier-integrated 50 GHz EML operating in the O-band, and a digital signal processor to compensate for CD-induced distortion [4,31]. This suggests that beyond-10G-class TDM-PONs may enable the allocation of the C-band for QKD, where propagation loss is minimal, provided that legacy 10G-class PONs are no longer in use. Adequate spectral separation between QKD and PON signals can help mitigate noise from Raman scattering [9]. However, spontaneous

Raman scattering generated by O-band PON signals remains non-negligible, given that high-power transmitters are required for beyond-10G-class TDM-PONs.

2.2. WDM- and TWDM-PON

The intensity modulation and direct detection (IM/DD)-based TDM-PON is expected to face significant challenges in meeting the required power budget, primarily due to power splitter-induced losses [2]. WDM-PON can address this issue, as shown in Figure 2a. For DS transmission in WDM-PON, the power budget requirement can be reduced, as the insertion loss of a WDM demultiplexer does not scale with the number of ONUs. This improved power margin enables the use of higher order modulation schemes, such as 4-level pulse-amplitude modulation, to increase line rates [7,32]. Furthermore, ONUs can operate at the full bit rate of a wavelength, as they receive a continuous signal. The ability to detect continuous signals also benefits low-latency applications, such as 5G fronthaul [1,19]. However, the high cost and complexity of WDM-PON remain the main obstacles to its widespread adoption. Each ONU in WDM-PON utilizes expensive wavelength-tunable lasers. Additionally, the use of a WDM demultiplexer for signal distribution establishes a fixed wavelength connection between the OLT and each ONU, posing operational challenges for network management. Efforts to mitigate these challenges have focused on colorless ONU transmitters, such as reflective semiconductor optical amplifiers (RSOAs), but these solutions still face difficulties in supporting high-bandwidth applications [32].

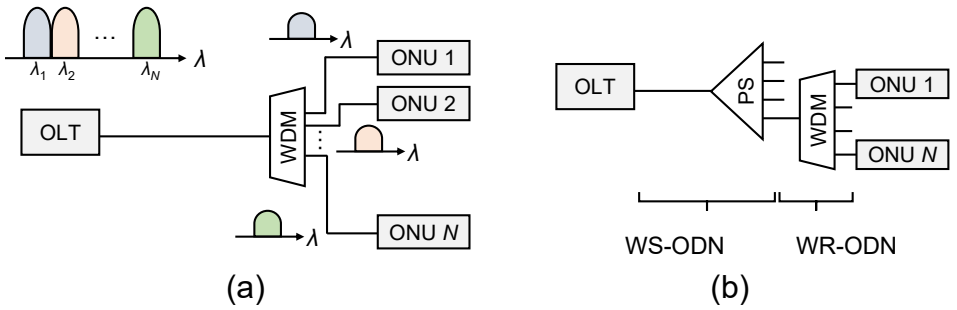

Figure 2. Schematic diagrams of (**a**) WDM-PON and (**b**) TWDM-PON employing a hybrid architecture of WS- and WR-ODNs.

To alleviate the wavelength management burden of WDM, a TWDM scheme has been proposed for the NG-PON2, transmitting four wavelength channels of 10G-class TDM-PON signals, as specified in ITU-T G.989 [2]. Figure 2b illustrates the structure of NG-PON2, which integrates wavelength-selected (WS) and wavelength-routed (WR) optical distribution networks (ODNs) [33]. This hybrid approach ensures compatibility with legacy TDM-PONs while reducing power budget requirements compared to a WS-only structure. When NG-PON2 was initially proposed, components operating above 10 GHz were not yet mature enough to implement a 40G-class PON [5]. However, it is likely that 50G-class PONs will continue to utilize the TDM scheme, as high-bandwidth components are expected to become commercially available [4,5,31]. Nevertheless, a WDM or TWDM scheme may be reintroduced for beyond-50G-class PONs to further scale capacity. Although NG-PON2 allocates the C- and L-bands for US and DS transmission, respectively, beyond-50G-class IM/DD-based WDM or TWDM-PONs are expected to operate in the O-band, as the line rate per wavelength is projected to exceed 25 Gb/s (in line with TDM-based bandwidth constraints [4]). Consequently, future high-speed PONs could allocate the C-band for QKD signaling, even when TWDM or WDM architectures are employed [1]. If the TDM architecture is to be used, an evolution toward coherent-lite PONs can be expected, as coherent receivers offer improved receiver sensitivity [8].

3. Case Study on QKD in P2MP Topology

3.1. Time-Bin-Encoded Discrete-Variable (DV)-QKD with GPON

Figure 3a shows the schematic diagram of a US DV-QKD system in a P2MP topology, designed to reduce the cost associated with QKD receivers [14]. Each QKD transmitter sends its key information over designated time slots, while the QKD receiver detects time-interleaved QKD signals. The configuration of QKD transmitters and receivers varies depending on the specific QKD protocol implemented. For instance, Figure 3b and Figure 3c illustrate the BB84 [34] and coherent one-way (COW) [35] protocols, respectively.

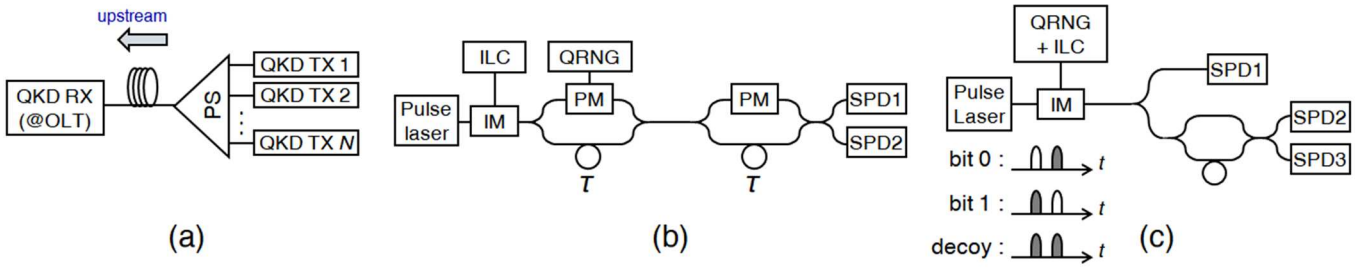

Figure 3. (**a**) Systematic configuration of US DV-QKD in P2MP topology. Setup for time-bin-encoded (**b**) BB84 and (**c**) COW protocols (ILC: intensity level controller, IM: intensity modulator, PM: phase modulator, QRNG: quantum random noise generator).

The feasibility of US QKD was experimentally demonstrated in a 20 km P2MP network comprising 4.4 km of feeder fiber and either 15.5 km or 11.8 km of drop fiber under dark fiber conditions [14]. In this experiment, the time-bin-encoded BB84 protocol was adopted. Although the OAN was assumed to accommodate eight subscribers using a 1×8 power splitter, only two QKD signals were transmitted to an OLT in the experiment. When two time slots out of eight were used, approximately 1% quantum bit error rates (QBERs) were achieved. However, an increase in QBERs was observed as crosstalk increased due to the reduced time slot interval between the two allocated subscribers. Consequently, it needs to be further demonstrated whether a QBER with an acceptable secret key rate can be achieved when all eight subscribers transmit QKD signals simultaneously (i.e., when the time slot interval is minimized among all subscribers).

The feasibility of the time-bin-encoded BB84-based QKD was investigated in a GPON environment [36]. Since US and DS GPON signals operate in the O-band and S-band, respectively, the QKD signal was transmitted at 1550 nm (i.e., within the C-band region). The optical spectrum was then measured at the OLT side (by tapping part of the power) to identify the major noise source [36]. The launched powers of the US and DS GPON signals were 4 dBm and 1 dBm, respectively. The feeder and drop fiber lengths were 15.5 km and 4.4 km, respectively. The results indicated that the noise was primarily influenced by the DS GPON signal [36], likely due to the smaller wavelength difference between the QKD and the DS GPON signal compared to the US GPON signal [9]. The feasibility of the QKD-integrated GPON system was evaluated based on the secret key rates, which were calculated from the experimental parameters. The following conditions were assumed:

- Total fiber length (feeder + drop fiber): 20 km;
- Launched DS GPON signal: −3 dBm;
- Number of ONUs: 8;
- Use of single photon detector (SPD) operating at 1 GHz with 26% efficiency.

Under these conditions, the feeder fiber length needed to remain below 8 km, as longer feeder fibers resulted in increased Raman backscattering from the DS GPON signals. Although reducing DS signal power could mitigate this issue [36,37], this approach is not viable for 10G or beyond-10G-class PON systems, which require higher launched power

levels. The inherent splitting loss in TDM-PONs poses additional challenges in scaling the number of ONUs. To mitigate Raman scattering, a dual feeder fiber scheme was proposed, wherein the $1 \times N$ power splitter at the cabinet side was replaced with a $2 \times N$ power splitter to separate the DS GPON signal path from the QKD signal reception path. However, this scheme required additional fiber for QKD, leading to increased costs.

Recently, the integration of QKD with the COW protocol and GPON was experimentally demonstrated, where US QKD was implemented, as shown in Figure 4a [9]. Since Raman backscattering from the DS GPON signal was the primary noise source for the QKD signal, the launched power of the DS GPON signal was adjusted to ensure a received power of −25 dBm (i.e., receiver sensitivity level). Without a feeder fiber, where the Raman scattering effects were minimal, the QKD operation was feasible for $N \leq 32$, as shown in Figure 4b. These experimental results were obtained for an OAN consisting solely of drop fiber with a 1 km reach. Figure 4b illustrates a significant decrease in the secret key rate with increasing N, primarily due to splitting loss. This suggests that the TDM scheme was unsuitable for QKD signal distribution. The effects of Raman scattering from the DS GPON signal were further analyzed in Figure 4c. When N increased from 2 to 4, the secret key rate decreased from 3.0 kbps to 1.2 kbps in the absence of a feeder fiber. When N is fixed to 2, a 13.4 km feeder fiber, inducing 2.6-dB loss, resulted in a secret key rate of 1.24 kbps. The 2.68-dB fiber loss was lower than the increased splitting loss of 3.6 dB observed when the splitting ratio increased from 2 to 4, potentially due to Raman backscattering from the DS GPON signal. For N = 16, even a 0.6 km feeder fiber induced effects comparable to those observed when doubling N without a feeder fiber. In this scenario, the launched power of the DS GPON signal needed to be increased to −3.4 dBm, leading to a higher Raman backscattering noise.

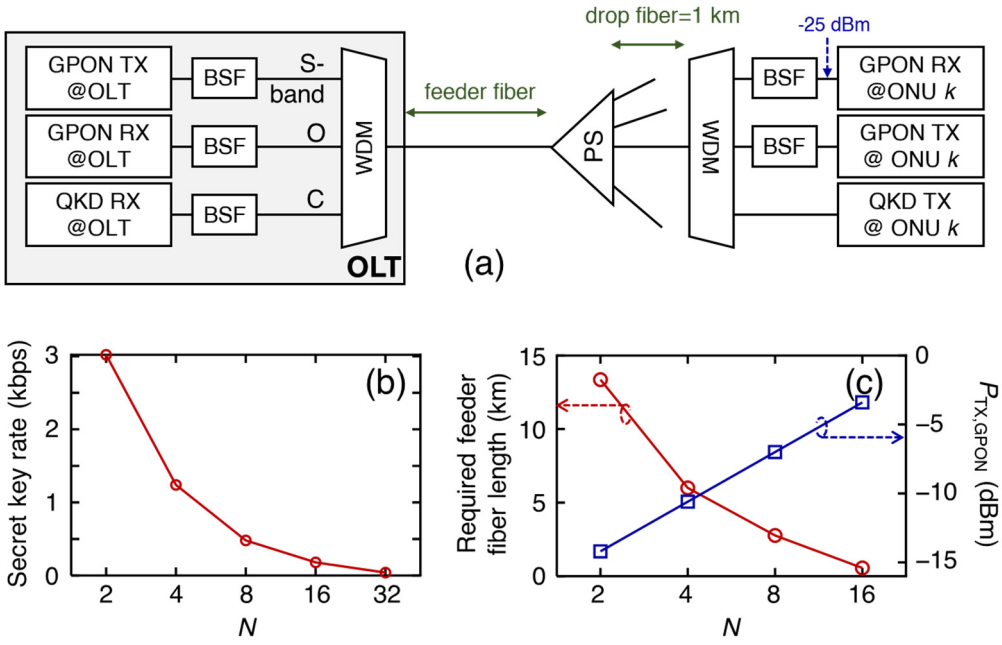

Figure 4. (**a**) Configuration of a QKD-integrated GPON (BSF: band-stop filter). (**b**) Secret key rate as a function of the number of ONUs without a feeder fiber. (**c**) Required feeder fiber length to achieve the same secret key rate as that obtained when increasing the number of ONUs from N to $2N$ in the absence of a feeder fiber. (**b**,**c**) are plotted based on the data in [9].

Since DV-QKD is highly sensitive to Raman scattering, it requires a large wavelength separation from PON signals. Consequently, DV-QKD cannot be seamlessly integrated with legacy PON systems operating in the S- or C-band. Although higher speed PONs (e.g., 25G- or 50G-class PONs) would operate only in the O-band to mitigate CD penalties, the US

DV-QKD remains incompatible with TDM-PONs due to its susceptibility to high splitting loss. The increased splitting loss necessitates a higher launched power for the PON signal, further exacerbating the Raman scattering effects on DV-QKD. Additionally, crosstalk from time-interleaved QKD signals transmitted by different ONUs presents another major challenge to seamless QKD integration within PON systems.

3.2. CV-QKD with PONs

While US QKD offers advantages in terms of reducing the number of QKD receivers, it introduces challenges in time-interleaving QKD signals from different ONUs, which can lead to crosstalk [36,38]. In contrast, CV-QKD leverages commercially available coherent receivers, enabling DS QKD and thereby reducing crosstalk-related performance degradation. By assigning a wavelength distinct from PON signals, a TDM-based DS QKD system can be implemented, as depicted in Figure 5a. Even though an OLT transmits QKD signals to all connected ONUs in this architecture, the security among ONUs is maintained [38]. An example of a CV-QKD system is illustrated in Figure 5b [39]. In this setup, a CV-QKD signal is transmitted according to the GG02 protocol [22] over a 202.81 km SSMF with a total loss of 32.45 dB [39]. Given that PONs typically require a power budget exceeding 29 dB for a 20 km transmission distance (i.e., a total loss of >33 dB) [5], this suggests that a TDM-based QKD access network can feasibly be implemented. In this 202.81 km transmission experiment, the QKD receiver was implemented using homodyne detection (which detects a single quadrature via a balanced photodetector) [22] and a transmitted local oscillator (TLO) scheme [40].

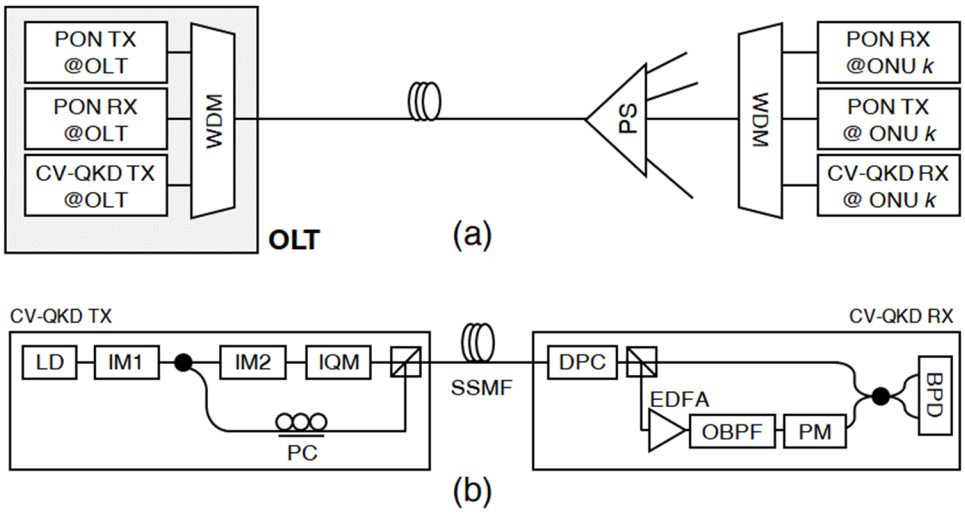

Figure 5. (**a**) Configuration of DS CV-QKD integrated with PON. (**b**) Exemplary setup for CV-QKD with GG02 protocol (BPD: balanced photodiode, DPC: dynamic polarization controller, EDFA: erbium-doped fiber amplifier, IQM: in-phase and quadrature modulator, LD: laser diode, OBPF: optical bandpass filter).

The experiments in [38] were conducted without the presence of PON signals, meaning that excess noise induced by crosstalk and Raman scattering was not considered [38]. However, excess noise increases when QKD is multiplexed with PON signals. The tolerable excess noise was analyzed in [38], showing that for a 10 km link, the acceptable excess noise decreased from 0.14 shot noise units (SNU) to 0.04 SNU, as shown in Figure 6. For a 20 km link, the tolerable excess noise was slightly reduced to 0.11 SNU. A group at Telecom ParisTech successfully demonstrated a CV-QKD system operating alongside a classical communication system over a 25 km link [41]. This demonstration is particularly relevant, as it falls within the typical PON reach. In their experiment, classical dense-WDM (DWDM)

signals and CV-QKD signals were multiplexed within the C-band, with a wavelength separation of just 20 nm. Their results indicated that the sum of excess noise and the photodetector's thermal noise remained below 0.11 SNU, which is within the acceptable range for a 20 km TDM-based quantum access network supporting four ONUs, provided that the launched power of the DS and US signals was kept below 4.7 dBm.

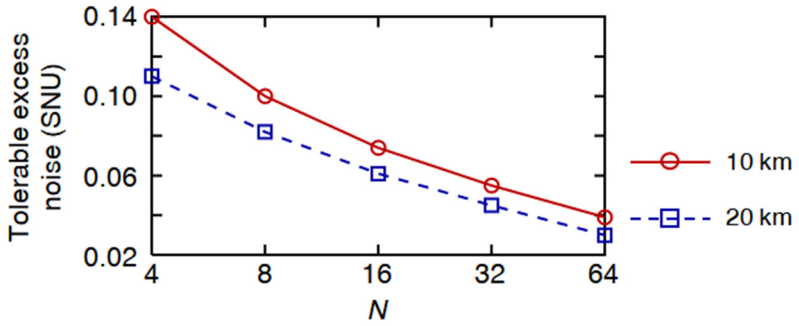

Figure 6. Tolerable excess noise in TDM-based CV-QKD as a function of the number of ONUs. The calculated data are obtained from [38].

Since the spectral separation between the QKD and classical signals in this experiment was only 20 nm, it can be inferred that QKD signals can also be transmitted in the L-band, coexisting with legacy PON signals operating in the O-, S-, and L-bands. Moreover, if the spectral separation between QKD and PON signals is increased, the launched power of PON signals can also be raised without significantly affecting QKD performance. Further improvements in scalability can be achieved by multiplexing QKD signals in the wavelength domain [42]. In one experiment, 194 CV-QKD signals were multiplexed using 25 GHz channel spacing, resulting in an excess noise per channel of less than 0.02 SNU. The crosstalk-induced excess noise was also inferred to be significantly below 0.02 SNU, indicating that WDM CV-QKD is a promising approach for future large-scale QKD-PONs.

4. Integration of CV-QKD Protocol in OANs

Current OANs are primarily implemented by TDM-PONs and are expected to evolve toward TWDM-PONs in the future. Therefore, a QKD system integrated into OANs needs to be capable of operating in a TDMA environment with a power splitter. In the case of DV-QKD, the high cost of SPDs necessitates the adoption of a US transmission structure, inherently limiting the system to serving a maximum of two end users while maintaining a transmission distance of 10 km or more, as shown in Figure 4b. This configuration is feasible only if the launched power of the GPON signal is minimized to meet the receiver sensitivity requirement—a condition unattainable in beyond-10G PON systems. Furthermore, implementing a US-based DV-QKD system necessitates a complex scheduling algorithm, posing additional challenges to practical deployment. In contrast, CV-QKD offers a more viable solution for OANs. Leveraging commercially available off-the-shelf optical receivers, CV-QKD enables TDMA, making it a practical and cost-effective approach for secure quantum communication in OANs. Therefore, this section focuses on CV-QKD and explores its suitability for seamless integration with next-generation OANs.

4.1. Architecture for DS CV-QKD-Integrated PONs

Figure 7 illustrates the architecture of a CV-QKD-integrated PON. Since PON systems operating at line rates up to 50 Gb/s are expected to utilize the O-, S-, and C-bands, the CV-QKD signals can be allocated in the L-band, where fiber loss is low and sufficient wavelength separation from PON signals is ensured. At the OLT, a QKD transmitter, a PON transmitter, and a receiver can be multiplexed in the wavelength domain. By

employing a DS transmission structure for QKD signals, the secret keys can be broadcast to multiple users through TDM. This approach not only facilitates efficient multi-user access but also minimizes crosstalk during key distribution to end users. After transmission through the feeder fiber, QKD signals are distributed to subscribers via a power splitter. A WDM filter then separates the PON US and DS signals from the QKD signal, ensuring minimal interference. In this architecture, CV-QKD signals can be implemented using a local LO (LLO) scheme [43], which allows for the extraction of the desired wavelength components with high frequency selectivity. Consequently, the LLO scheme is a promising approach for mitigating interference and enhancing the stability of CV-QKD integration in next-generation PONs.

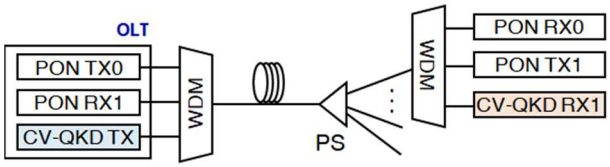

Figure 7. Configuration of DS CV-QKD-integrated PON.

4.2. CV-QKD Implementation Technique

This section examines various implementation methods for CV-QKD. A summary of previously demonstrated CV-QKD systems is provided in Table 2, while the following subsections analyze the key modules in detail.

Table 2. CV-QKD implementation.

Authors	Laser	Modulation	LO/Pilot (Multiplexing)	Distance (km)	Polarization Tracking	Optical Receiver	SKR
J. Lodewyck et al. [40]	Pulse (350 kHz)	Gaussian (AM+PM)	TLO (TDM+PDM)	25	MPC	Homodyne	20 kbps
P. Jouget et al. [44]	Pulse (1 MHz)	Gaussian (AM+PM)	TLO (TDM+PDM)	80	DPC	Homodyne	0.2 kbps
D. Huang et al. [45]	Pulse (10 MHz)	Gaussian (AM+PM)	TLO (TDM+PDM)	25	DPC	Homodyne	1 Mbps
Y. Zhang et al. [39]	Pulse (5 MHz)	Gaussian (AM+PM)	TLO (TDM+PDM)	202.81	DPC	Homodyne	6.214 bps
S. Ren et al. [43]	Pulse (500 MHz)	Gaussian (AM+PM)	Pseudo LLO (TDM)	15	MPC	Heterodyne	26.9 Mbps
H. Wang et al. [46]	CW	QPSK (IQM)	LLO (TDM)	25	DPC	Heterodyne	52.48 Mbps
D. Pereira et al. [47]	CW	PCS-128APSK (IQM)	LLO	40	DSP	Heterodyne	1.2 Mbps
N. Jain et al. [48]	CW	Gaussian (IQM)	LLO (FDM)	20	DSP	Heterodyne	4.71 Mbps

4.2.1. LO or Pilot

Each symbol of a CV-QKD signal is in a coherent state and requires an LO for detection. To compensate for phase noise in the laser generating the QKD signal, an interference scheme using the same laser at the transmitter is employed, known as the TLO scheme [40]. Since the signal-to-noise ratio (SNR) of the received signal is proportional to the LO power, a high-power TLO must be transmitted. However, TLO experiences attenuation during fiber transmission, potentially necessitating an additional optical amplifier at the receiver [39]. While an erbium-doped fiber amplifier (EDFA) can reduce excess noise compared to a semiconductor optical amplifier (SOA), it is expensive and occupies significant space, making it less suitable for OANs. Moreover, the TLO induces a security loophole, as Eve

can manipulate the LO [43]. Alternatively, using an independent laser at the receiver as the LO is known as the LLO scheme. In this case, the optical signal transmitted from the source laser for phase noise tracking is called the pilot. Unlike TLO, which requires high power, the pilot signal is transmitted with just enough power for phase estimation and compensation.

Both CV-QKD signals and LO (or pilot) must be transmitted simultaneously, employing various multiplexing techniques such as TDM, polarization-division multiplexing (PDM), and frequency-division multiplexing (FDM) [39,40,43–48]. Typically, TDM is used with the TLO scheme, where QKD signals and TLO are placed in orthogonal polarizations to prevent interference-induced beat components. In contrast, when LLO is used, the QKD signals and the pilot are typically transmitted via FDM, as they do not require direct interference for detection.

4.2.2. Laser Source

When LO or pilot is multiplexed with QKD signals in the time domain, a pulsed laser must be used. The pulsed laser utilized in CV-QKD does not require a high repetition rate or ultra-narrow pulse widths. Consequently, continuous-wave (CW) lasers modulated by an MZM are commonly used to generate the required pulses [39,40,43–45]. In TLO-based CV-QKD systems, the LO power must be significantly higher than that of the QKD signal. Typically, an LO signal contains 10^4–10^8 photons per pulse, whereas a QKD signal contains fewer than 20 photons [49]. Due to this large disparity, the extinction ratio (ER) of the pulse must be extremely high to minimize LO-induced interference with the QKD signal. An ER of 80 dB ER has been reported using a cascaded dual-MZM configuration [50]. However, achieving such a high ER becomes increasingly difficult as the repetition rate increases. If QKD and TLO (or pilot) are not time-multiplexed, CW lasers can be used directly, eliminating the need for pulse generation and thereby enhancing the secret key rate of CV-QKD.

4.2.3. Modulation and Modulator

Gaussian modulation is the most commonly used scheme for CV-QKD as it enables a high secret key rate. However, it requires high-resolution digital-to-analog converters (DACs) and analog-to-digital converters (ADCs) and complex reconciliation algorithms, posing a significant challenge. To address these limitations, discrete modulation techniques such as phase shift keying (PSK) and quadrature amplitude modulation (QAM) have been proposed [46–48]. Lower modulation levels allow for low-resolution DACs and ADCs, reducing complexity and making the system more cost-effective for OANs. To increase the secret key rate, higher order modulation levels or probabilistic constellation shaping (PCS) can be adopted [47]. In PCS, the probability mass function of modulation levels follows a Gaussian distribution, but the number of discrete levels is limited, enabling a compromise between Gaussian and discrete modulation schemes.

An IQ modulator can be used to generate the CV-QKD signals. When implementing the GG02 protocol, independent Gaussian-distributed electrical signals are applied to the I- and Q-axes. IQ modulators offer improved tolerance to overshooting or ringing in the driving signals [51]. An alternative approach involves cascading an amplitude modulator (AM) and a phase modulator (PM) in series. For the GG02 protocol, a Rayleigh-distributed electrical signal is applied to the AM, and a uniformly distributed signal is applied to the PM. This approach is more cost-effective and introduces lower loss than an IQ modulator. However, when detecting either IQ quadrature, the resolution of the PM signal may vary depending on the AM modulation levels, which is a drawback of this approach.

4.2.4. Polarization Tracking or Demultiplexing

In optical fiber transmission, the vertical and horizontal polarization modes are degenerate, leading to time-varying polarization mismatches between the transmitted and received signals. Since CV-QKD detection requires precise polarization alignment between the LO and QKD signals, polarization tracking becomes essential. If the QKD signals and LO (or pilot) are transmitted in different polarization modes, a polarization demultiplexing technique needs to be employed. Inaccurate tracking induces increased excess noise. In laboratory conditions, manual polarization control (MPC) is sometimes used; however, for real-world deployment, dynamic polarization control (DPC) or digital signal processing (DSP)-based polarization tracking is required to ensure stability and reliability.

4.2.5. Optical Receiver

The GG02 protocol suggests that Alice modulates two quadratures using Gaussian modulation, while Bob randomly selects and measures one of the quadratures using homodyne detection [22]. Homodyne detection requires an optical coupler for combining the QKD and LO signals, a balanced photodetector (BPD) for measurement, and a phase modulator to lock the LO phase and select the measurement basis. Later research demonstrated that using heterodyne detection, where both quadratures are simultaneously measured, does not compromise security [52]. In heterodyne detection, the QKD signal and LO are mixed via an optical hybrid, and two BPDs are used for detection. This method introduces a 3 dB optical power penalty due to signal splitting but doubles the SKR. While homodyne detection may suffer from excess noise due to real-time phase locking errors, heterodyne detection allows for carrier phase estimation algorithms to compensate for phase noise, enhancing system performance.

4.3. Cost-Effective CV-QKD Implementation Integrated with OAN

Considering the cost-sensitive nature of OANs, CV-QKD must be designed with cost efficiency in mind. To reduce complexity, low-order discrete modulation schemes (e.g., QPSK, 16-QAM) are preferable over Gaussian modulation, as they require lower resolution DACs and ADCs. Although this approach reduces the secret key rate, the accumulated secret keys over extended periods can still ensure secure communication. LLO-based CV-QKD is considered more suitable for OANs. The TDMA scheme reduces the TLO power, directly degrading the SNR of the detected signal. While EDFAs can be used to boost the TLO, their high cost and large footprint make them impractical for OANs. LLO eliminates the need for the TDM-based multiplexing of pilot and QKD signals, further reducing pulse generation costs. For detection, heterodyne measurement is preferable, since it can avoid precise phase locking, which is challenging to achieve in real-time.

5. Conclusions

In this paper, we reviewed the optical link design perspectives of QKD-integrated OAN systems, analyzing both technical feasibility and potential implementation challenges. First, we examined the evolution of PON technologies. In legacy PON systems operating at speeds up to 10G, US signals are transmitted in the O-band, while DS signals are transmitted in either the S- or C-band. The 25G and 50G PONs are expected to utilize only the O-band for both DS and US signals to mitigate CD penalties, and they require a high launched power. Secondly, we reviewed QKD implementations in P2MP topology. Implementing DV-QKD in OANs requires a US structure to minimize the number of expensive SPDs. However, for links exceeding 10 km, this approach can barely support two users—and even then, only if the PON signal launch power is significantly reduced. Such a condition is impractical for beyond-10G PON systems. As a result, CV-QKD emerges as a more suitable

alternative, offering simplified scheduling and reduced crosstalk in a multi-user secret key distribution. Among various CV-QKD architectures, the DS CV-QKD scheme is particularly advantageous for OAN integration due to its low crosstalk characteristics. Finally, we suggested the structural design of DS CV-QKD-integrated OAN systems and analyzed the key module configurations required for CV-QKD implementation. By reviewing the existing research, we assessed these configurations from a cost-effectiveness perspective, providing insights into practical deployment strategies for QKD-enabled OANs.

Author Contributions: Investigation, S.B.; supervision, S.-T.K. All authors have read and agreed to the published version of the manuscript.

Funding: This work was supported in part by 2024 Research Grant from Kangwon National University and in part by the Institute for Information and Communications Technology Planning & Evaluation (IITP)-Information Technology Research Center (ITRC) (No. RS-2024-00437191).

Institutional Review Board Statement: Not applicable.

Informed Consent Statement: Not applicable.

Data Availability Statement: The data presented in this study are available on request from the corresponding author.

Conflicts of Interest: The authors declare no conflicts of interest.

References

1. Wey, J. The outlook for PON standardization: A tutorial. *J. Lightwave Technol.* **2020**, *38*, 31–42. [CrossRef]
2. Nesset, D. NG-PON2 Technology and Standards. *J. Lightwave Technol.* **2015**, *33*, 1136–1143. [CrossRef]
3. Houtsma, V.; van Veen, D.; Harstead, E. Recent progress on standardization of next-generation 25, 50, and 100G EPON. *J. Lightwave Technol.* **2017**, *35*, 1228–1234. [CrossRef]
4. Zhang, D.; Liu, D.; Wu, X.; Nesset, D. Progress of ITU-T higher speed passive optical network (50G-PON) standardization. *J. Opt. Commun. Netw.* **2020**, *12*, D99–D108. [CrossRef]
5. Houtsma, V.; Mahadevan, A.; Kaneda, N.; van Veen, D. Transceiver technologies for passive optical networks: Past, present, and future. *J. Opt. Commun. Netw.* **2021**, *13*, A44–A55. [CrossRef]
6. Zhu, Y.; Yi, L.; Yang, B.; Huang, X.; Wey, J.; Ma, Z.; Hu, W. Comparative study of cost-effective coherent and direct detection schemes for 10 Gb/s/λ PON. *J. Opt. Commun. Netw.* **2020**, *12*, D36–D47. [CrossRef]
7. Che, Y.; Kim, H. Cost-effective C-band 50-Gb/s PON implemented by using a 2-bit DAC and linear electrical equalizer. *IEEE Photonics Technol. Lett.* **2023**, *35*, 215–218. [CrossRef]
8. Moon, S.-R.; Bae, S. Coherent-lite PON with repetition code and single polarization receiver. *Opt. Comm.* **2024**, *557*, 130331–130336. [CrossRef]
9. Zavitsanos, D.; Ntanos, A.; Stathopoulos, T.; Raptakis, A.; Setaki, F.; Lyberopoulos, G.; Kouloumentas, C.; Giannoulis, G.; Avramopoulos, H. Feasibility analysis of QKD integration in real-world FTTH access networks. *J. Lightwave Technol.* **2024**, *42*, 4–11. [CrossRef]
10. *ITU-T G.9807.1*; 10-Gigabit-Capable Symmetric Passive Optical Network (XGS-PON). ITU: Geneva, Switzerland, 2023.
11. *ITU-T G.9804.1*; Higher Speed Passive Optical Networks: Requirements. ITU: Geneva, Switzerland, 2019.
12. *ITU-T G.Sup64 Supplement*; PON Transmission Technologies Above 10 Gbit/s Per Wavelength. ITU: Geneva, Switzerland, 2018.
13. Atan, F.; Zulkifli, N.; Idrus, S.; Ismail, N.; Zin, A.; Ramli, A.; Yusoff, N. Security enhanced dynamic bandwidth allocation algorithm against degradation attacks in next generation passive optical networks. *J. Opt. Commun. Netw.* **2021**, *13*, 301–311. [CrossRef]
14. Frohlich, B.; Dynes, J.; Lucamarini, M.; Sharpe, A.; Yuan, Z.; Shields, A. A quantum access network. *Nature* **2013**, *501*, 69–74. [CrossRef] [PubMed]
15. Cao, Y.; Zhao, Y.; Wang, Q.; Zhang, J.; Ng, S.X.; Hanzo, L. The Evolution of Quantum Key Distribution Networks: On the Road to the Qinternet. *IEEE Commun. Surv. Tutor.* **2022**, *24*, 839–894. [CrossRef]
16. Ntanos, A.; Zavitsanos, D.; Giannoulis, G.; Avramopoulos, H. QKD in Support of Secured P2P and P2MP Key Exchange for Low-Latency 5G Connectivity. In Proceedings of the 2020 IEEE 3rd 5G World Forum (5GWF), Bangalore, India, 10–12 September 2020; pp. 157–162.
17. Chowdhury, A.; Karmakar, G.; Kamruzzaman, J.; Jolfaei, A.; Das, R. Attacks on Self-Driving Cars and Their Countermeasures: A Survey. *IEEE Access* **2020**, *8*, 207308–207342. [CrossRef]

18. Fayad, A.; Cinkler, T.; Rak, J. Toward 6G Optical Fronthaul: A Survey on Enabling Technologies and Research Perspectives. *IEEE Commun. Surv. Tutor.* **2025**, *27*, 629–666. [CrossRef]
19. Effenberger, F.J.; Zhang, D. WDM-PON for 5G Wireless Fronthaul. *IEEE Wirel. Commun.* **2022**, *29*, 94–99. [CrossRef]
20. Chung, H.; Lee, H.H.; Kim, K.O.; Doo, K.-H.; Ra, Y.; Park, C. TDM-PON-Based Optical Access Network for Tactile Internet, 5G, and Beyond. *IEEE Netw.* **2022**, *36*, 76–81. [CrossRef]
21. Shor, P.W.; Preskill, J. Simple proof of security of the BB84 quantum key distribution protocol. *Phys. Rev. Lett.* **2000**, *85*, 441–444. [CrossRef]
22. Grosshans, F.; Grangier, P. Continuous variable quantum cryptography using coherent states. *Phys. Rev. Lett.* **2002**, *5*, 057902. [CrossRef] [PubMed]
23. Eriksson, T.; Hirano, T.; Puttnam, B.; Rademacher, G.; Luis, R.; Fujiwara, M.; Namiki, R.; Awaji, Y.; Takeoka, M.; Wada, N.; et al. Wavelength division multiplexing of continuous variable quantum key distribution and 18.3 Tbit/s data channels. *Commun. Phys.* **2019**, *2*, 9. [CrossRef]
24. 10 Gb/s Ethernet Passive Optical Network. IEEE P802.3av Task Force. Available online: https://www.ieee802.org/3/av/ (accessed on 14 October 2009).
25. Harstead, E.; Powell, B. 25G/50G/100G EPON Architectures: 1+3 vs. 1+4. Presented at the IEEE 802.3CA Meeting, Fort Worth TX, USA, 13–15 September 2016. Available online: https://www.ieee802.org/3/ca/public/meeting_archive/2016/09/harstead_3ca_1a_0916.pdf (accessed on 13 September 2016).
26. *G.984.2*; Gigabit-Capable Passive Optical Networks (GPON): Physical Media Dependent (PMD) Layer Specification. ITU-T: Geneva, Switzerland, 2008. Available online: https://www.itu.int/rec/T-REC-G.984.2-201908-I/en (accessed on 22 April 2025).
27. *IEE P802.3ah*; Ethernet in the First Mile Task Force. IEEE: Piscataway, NJ, USA, 2011. Available online: https://www.ieee802.org/3/efm/ (accessed on 22 April 2025).
28. *G.987.2*; 10-Gigabit-Capable Passive Optical Networks (XG-PON): Physical Media Dependent (PMD) Layer Specification. ITU-T: Geneva, Switzerland, 2023. Available online: https://www.itu.int/rec/T-REC-G.987.2/en (accessed on 22 April 2025).
29. *IEEE 802.3ca*; IEEE Standard for Ethernet Amendment 9. IEEE: Piscataway, NJ, USA, 2020. Available online: https://standards.ieee.org/ieee/802.3ca/7440/ (accessed on 22 April 2025).
30. *G.989.2*; 40-Gigabit-Capable Passive Optical Networks 2 (NG-PON2): Physical Media Dependent (PMD) Layer Specification. ITU-T: Geneva, Switzerland, 2019. Available online: https://www.itu.int/rec/T-REC-G.989.2/en (accessed on 22 April 2025).
31. Bonk, R.; Geng, D.; Khotimsky, D.; Liu, D.; Liu, X.; Luo, Y.; Nesset, D.; Oksman, V.; Strobel, R.; Hoof, W.; et al. 50G-PON: The First ITU-T Higher-Speed PON System. *IEEE Comm. Mag.* **2022**, *60*, 48–54. [CrossRef]
32. Shim, H.; Kim, H.; Chung, Y. Effects of Electrical and Optical Equalizations in 28-Gb/s RSOA-Based WDM PON. *IEEE Photon. Technol. Lett.* **2016**, *28*, 2537–2540. [CrossRef]
33. Wey, J.; Nesset, D.; Valvo, M.; Grobe, K.; Roberts, H.; Luo, Y.; Smith, J. Physical layer aspects of NG-PON2 standards—Part 1: Optical link design. *J. Opt. Commun. Netw.* **2020**, *8*, 33–42. [CrossRef]
34. Townsend, P.; Rarity, J.; Tapster, P. Single photon interference in 10 km long optical fibre interferometer. *Electron. Lett.* **1993**, *29*, 634–635. [CrossRef]
35. Stucki, D.; Brunner, N.; Gisin, N.; Scarani, V.; Zbinden, H. Fast and simple one-way quantum key distribution. *Appl. Phys. Lett.* **2005**, *87*, 194108–194111. [CrossRef]
36. Frohlich, B.; Dynes, J.; Lucamarini, M.; Sharpe, A.; Tam, S.; Yuan, Z.; Shields, A. Quantum secured gigabit optical access networks. *Sci. Rep.* **2016**, *5*, 18121. [CrossRef]
37. Patel, K.; Dynes, J.; Choi, I.; Sharpe, A.; Dixon, A.; Yuan, Z.; Penty, R.; Shields, A. Coexistence of high-bit-rate quantum key distribution and data on optical fiber. *Phys. Rev. X* **2012**, *2*, 041010. [CrossRef]
38. Huang, Y.; Shen, T.; Wang, X.; Chen, Z.; Xu, B.; Yu, S.; Guo, H. Realizing a downstream-access network using continuous-variable quantum key distribution. *Phys. Rev. Appl.* **2021**, *16*, 064051. [CrossRef]
39. Zhang, Y.; Chen, Z.; Pirandola, S.; Wang, X.; Zhou, C.; Chu, B.; Zhao, Y.; Xu, B.; Yu, S.; Guo, H. Long-distance continuous-variable quantum key distribution over 202.81 km of fiber. *Phys. Rev. Lett.* **2020**, *125*, 010502. [CrossRef]
40. Lodewyck, J.; Bloch, M.; Patron, R.; Fossier, S.; Karpov, E.; Diamanti, E.; Debuisschert, T.; Cerf, N.; Brouri, R.; McLaughlin, S.; et al. Quantum key distribution over 25 km with an all-fiber continuous-variable system. *Phys. Rev. A* **2007**, *76*, 042305. [CrossRef]
41. Kumar, R.; Qin, H.; Alleaume, R. Coexistence of continuous variable QKD with intense DWDM classical channels. *New J. Phys.* **2015**, *17*, 043027. [CrossRef]
42. Eriksson, T.; Luis, R.; Puttnam, B.; Rademacher, G.; Fujiwara, M.; Awaji, Y.; Furukawa, H.; Wada, N.; Takeoka, M.; Sasaki, M. Wavelength division multiplexing of 194 continuous variable quantum key distribution channels. *J. Lightwave Technol.* **2020**, *38*, 2214–2218. [CrossRef]
43. Ren, S.; Yang, S.; Wonfor, A.; White, I.; Penty, R. Demonstration of high-speed and low-complexity continuous variable quantum key distribution system with local local oscillator. *Sci. Rep.* **2021**, *11*, 9454. [CrossRef] [PubMed]

44. Jouget, P.; Jacques, S.; Leverrier, A.; Grangier, P. Experimental demonstration of long-distance continuous-variable quantum key distribution. *Nat. Photonics* **2013**, *14*, 378–381. [CrossRef]
45. Huang, D.; Lin, D.; Wang, C.; Liu, W.; Fang, S.; Peng, J.; Huang, P.; Zeng, G. Continuous-variable quantum key distribution with 1 Mbps secure key rate. *Opt. Express* **2015**, *23*, 17511–17519. [CrossRef]
46. Wang, H.; Li, Y.; Pi, Y.; Pan, Y.; Shao, Y.; Ma, L.; Zhang, Y.; Yang, J.; Zhang, T.; Huang, W.; et al. Sub-Gbps key rate four-state continuous-variable quantum key distribution within metropolitan area. *Commun. Phys.* **2022**, *5*, 162. [CrossRef]
47. Pereira, D.; Almeida, M.; Facao, M.; Pinto, A.; Silva, N. Probabilistic shaped 128-APSK CV-QKD transmission system over optical fibres. *Opt. Lett.* **2022**, *47*, 3948–3951. [CrossRef] [PubMed]
48. Jain, N.; Chin, H.-M.; Mani, H.; Lupo, C.; Nikolic, D.S.; Kordts, A.; Pirandola, S.; Pedersen, T.B.; Kolb, M.; Ömer, B.; et al. Practical continuous-variable quantum key distribution with composable security. *Nat. Commun.* **2022**, *13*, 4740. [CrossRef]
49. Zhang, Y.; Bian, Y.; Li, Z.; Yu, S.; Guo, H. Continuous-variable quantum key distributionsystem: Past, present, and future. *Appl. Phys. Rev.* **2024**, *11*, 011318. [CrossRef]
50. Wang, X.; Liu, J.; Li, X.; Li, Y. Generation of stable and high extinction ratio light pulses for continuous variable quantum key distribution. *IEEE J. Quantum Electron.* **2015**, *51*, 5200206. [CrossRef]
51. Winzer, P.; Essiambre, R.-J. Advanced optical modulation formats. *Proc. IEEE* **2006**, *94*, 952–985. [CrossRef]
52. Weedbrook, C.; Lance, A.; Bowen, W.; Symul, T.; Ralph, T.; Lam, P. Quantum cryptography without switching. *Phys. Rev. Lett.* **2004**, *93*, 170504. [CrossRef] [PubMed]